



Reproducibility of [18F]FDG PET/CT liver SUV as reference or normalisation factor

Gerben J. C. Zwezerijnen^{1,2} · Jakoba J. Eertink^{2,3} · Maria C. Ferrández^{1,2} · Sanne E. Wiegers^{1,2} · Coreline N. Burggraaff³ · Pieterella J. Lugtenburg⁴ · Martijn W. Heymans^{5,6} · Henrica C. W. de Vet^{5,6} · José M. Zijlstra^{2,3} · Ronald Boellaard^{1,2}

Received: 9 August 2022 / Accepted: 15 September 2022
© The Author(s) 2022

Abstract

Introduction Although visual and quantitative assessments of [18F]FDG PET/CT studies typically rely on liver uptake value as a reference or normalisation factor, consensus or consistency in measuring [18F]FDG uptake is lacking. Therefore, we evaluate the variation of several liver standardised uptake value (SUV) measurements in lymphoma [18F]FDG PET/CT studies using different uptake metrics.

Methods PET/CT scans from 34 lymphoma patients were used to calculate SUV_{max}^{liver} , SUV_{peak}^{liver} and SUV_{mean}^{liver} as a function of (1) volume-of-interest (VOI) size, (2) location, (3) imaging time point and (4) as a function of total metabolic tumour volume (MTV). The impact of reconstruction protocol on liver uptake is studied on 15 baseline lymphoma patient scans. The effect of noise on liver SUV was assessed using full and 25% count images of 15 lymphoma scans.

Results Generally, SUV_{max}^{liver} and SUV_{peak}^{liver} were 38% and 16% higher compared to SUV_{mean}^{liver} . SUV_{max}^{liver} and SUV_{peak}^{liver} increased up to 31% and 15% with VOI size while SUV_{mean}^{liver} remained unchanged with the lowest variability for the largest VOI size. Liver uptake metrics were not affected by VOI location. Compared to baseline, liver uptake metrics were 15–18% and 9–18% higher at interim and EoT PET, respectively. SUV^{liver} decreased with larger total MTVs. SUV_{max}^{liver} and SUV_{peak}^{liver} were affected by reconstruction protocol up to 62%. SUV_{max} and SUV_{peak} moved 22% and 11% upward between full and 25% count images.

Conclusion SUV_{mean}^{liver} was most robust against VOI size, location, reconstruction protocol and image noise level, and is thus the most reproducible metric for liver uptake. The commonly recommended 3 cm diameter spherical VOI-based SUV_{mean}^{liver} values were only slightly more variable than those seen with larger VOI sizes and are sufficient for SUV_{mean}^{liver} measurements in future studies.

Trial registration EudraCT: 2006–005,174-42, 01–08-2008.

Keywords Liver uptake · Reference · VOI · [18F]FDG PET/CT

This article is part of the Topical Collection on Hematology

✉ Ronald Boellaard
r.boellaard@amsterdamumc.nl

Gerben J. C. Zwezerijnen
g.zwezerijnen@amsterdamumc.nl

¹ Radiology and Nuclear Medicine, Amsterdam UMC Location Vrije Universiteit Amsterdam, Amsterdam, The Netherlands

² Cancer Center Amsterdam, Imaging and Biomarkers, Amsterdam, The Netherlands

³ Amsterdam UMC Location Vrije Universiteit Amsterdam, Hematology, Amsterdam, The Netherlands

⁴ Erasmus MC Cancer Institute, University Medical Center, Hematology, Rotterdam, The Netherlands

⁵ Epidemiology and Data Science, Amsterdam UMC Location Vrije Universiteit Amsterdam, De Boelelaan 1117, Amsterdam, The Netherlands

⁶ Amsterdam Public Health Research Institute, Methodology, Amsterdam, The Netherlands

Introduction

^{18}F -fluoro-deoxy-glucose (^{18}F FDG) positron emission tomography-computed tomography (PET/CT) is widely used for diagnosis, staging, response prediction, and monitoring in oncology and lymphoma. In the majority of cases, clinical reads are based on visual assessment of ^{18}F FDG uptake and distribution in lesions and across the body [1]. Yet, quantitative ^{18}F FDG PET assessments have gained interest, with quantitative uptake measures such as standardised uptake values (SUV), metabolic tumour volume (MTV), or total lesion glycolysis (TLG) showing diagnostic, prognostic and predictive value for several oncological and haematological applications [2–4].

Both visual evaluation and quantitative assessments of ^{18}F FDG uptake require standardisation and harmonisation of the ^{18}F FDG PET/CT examinations in order to obtain reproducible results [5]. To this end, various scientific organisations have issued ^{18}F FDG PET/CT imaging procedural guidelines and set up PET/CT accreditation or validation programs to assure that PET-CT systems are calibrated correctly and that certain reconstruction protocols are applied to guarantee harmonised image qualities and quantitation [6–8]. Despite these efforts, ^{18}F FDG PET/CT may still suffer from several uncertainties. Consequently, the European Association of Nuclear Medicine (EANM) guideline recommends to assess liver SUV for quality control (QC) purposes of the patient's examination [6]. Mean liver SUV, derived from a 3-cm-diameter volume of interest (VOI) placed in the upper right lobe of the liver, as recommended by the EANM guideline, is expected to be within a range between SUV 1.3 and 3.0 [6]. A mean liver SUV outside this range may suggest errors in patient weight, injected activity or deviation in the performance of the PET/CT system. In case of visual reads, liver uptake is sometimes used as reference. For example, in lymphoma interim and end-of-treatment (EoT) PET studies, the so-called Deauville score is based on visually assessing whether and to what extent tumour uptake exceeds liver uptake (or mediastinal blood pool) [1, 9]. This assessment is used to classify tumour uptake into a 5-point score, which is subsequently used in clinical decision-making. Moreover, tumour contouring thresholds may be based on liver SUV, e.g. by taking the mean liver SUV times a factor as the SUV threshold to be used for lesion segmentation [10]. A similar approach is used by PERCIST to differentiate between target and non-target lesion for assessing treatment response using the mean liver SUV plus 2 standard deviations [11]. Thus, liver uptake is an important factor used for several purposes for both visual and quantitative ^{18}F FDG PET/CT reads.

There is, however, no consensus nor consistency in the way liver SUV is used. For QC purposes, the EANM, PERCIST, UPICT and SNMMI recommend to evaluate the

mean SUV in a 3-cm-diameter VOI placed in the upper right lobe of the (unaffected) liver. The ACRIN trial protocols recommend the use of liver SUV_{mean} calculated from a maximum region of interest (ROI) diameter in the liver [12]. In the approach for quantitative Deauville score at interim PET, is the lesion peak SUV (SUV_{peak}) compared with liver SUV_{mean} to derive the quantitative Deauville score [13]. Interestingly, for EoT PET/CT in lymphoma patients, lesion maximal SUV (SUV_{max}) is compared with liver SUV_{max} [1, 14]. Likewise, there is also lack of a consistent definition of SUV_{peak}, which is derived by using a 1-mL spherical VOI as per EANM, PERCIST, SNMMI and QIBA recommendations versus the use of a certain number of connected hottest voxels near the SUV_{max} [15]. Although one VOI and SUV metric definition may not necessarily be better than the other, they are different and thus might generate different uptake values. Supplementary Table 1 provides an overview of the various liver uptake assessment methodologies as will be discussed later in this paper.

The inconsistency in the definition of liver uptake and the use of various VOI definitions makes comparisons across studies, even before, during and after treatment within the same patient, difficult. Moreover, the use of SUV_{max} is under debate as it has been reported that it is prone to noise, showing increased upward bias with elevated noise levels, and is more sensitive to variations in image quality and reconstruction settings/protocols than SUV_{peak} and SUV_{mean} [16, 17].

The aim of this paper is therefore to perform an evaluation on the variation of several liver SUV uptake measurements arising from using different uptake metrics, different VOIs, different noise levels, at different time points across treatment (baseline, interim and EoT) and at different tumour loads. The paper will conclude by providing some recommendations for the use of liver SUV that will improve the robustness and reproducibility of liver SUV in multicentre studies and for comparisons between studies.

Methods

Patient datasets

In this study, three study datasets were used. The first dataset (dataset 1) consisted of 34 randomly selected patients with diffuse large B cell lymphoma (DLBCL) for whom baseline, interim and EoT scans were available from the HOVON-84 study (EudraCT2006-005,174–42, NTR1014) (Supplementary Table 2) [18]. Sites were instructed to perform the PET/CT studies following the EANM recommendation including a 4-h fasting status for patients before tracer administration,

a 60-min [18F]FDG uptake interval and use of EARL1 standards accredited PET/CT systems. More details of the HOVON-84 study are described previously [18]. The institutional review boards approved the study at all centers, and participants gave written informed consent before enrollment.

For the second dataset, we used $n = 15$ [18F]FDG PET/CT scans of lymphoma patients scanned at baseline in our institute using a Philips Ingenuity PET/CT system (Philips Healthcare, Cleveland, USA). The latter scans were collected consecutively from ongoing clinical investigations and the use of these (anonymised) data for technical scientific purposes was waived by the VU Medical Center ethics review board. The data was used previously and are described in Kaalep et al. [19]. This dataset is presently being used to explore the impact of different image reconstruction protocols on liver SUV. In short, PET scans were performed conform EANM recommendation using a bed scan duration of 2 min and an injected activity of 3 MBq/kg. Scans were reconstructed following protocols compliant with EARL-1 and 2 standards; both implemented with $4 \times 4 \times 4$ mm voxels. In addition, a locally preferred high-resolution reconstruction was included using $2 \times 2 \times 2$ mm voxels in combination with so-called point spread function (PSF) reconstructions [17]. As available on the PET/CT system, the vendor-provided reconstruction algorithm (called BLOB-OS-TF) was used to generate the reconstructed PET images.

Finally, a third dataset was generated to explore the impact of noise on liver SUV. For this dataset, we included $n = 15$ new [18F]FDG PET/CT studies of lymphoma patients scanned at baseline using the Philips Ingenuity PET/CT system (Philips Healthcare, Cleveland, USA). Data were taken from ongoing routine clinical investigations, and the use of the (anonymised) data for technical scientific purposes was waived by the VU Medical Center ethics review board. Two sets of reconstructions were made. First, we reconstructed the full count image data taking all the counts acquired during our standard 2 min per bed position acquisition protocol using a 3MBq/kg FDG activity prescription (scan duration = 120 s per bed). Next, for each bed position, we used only the counts collected during the first 30 s for each bed position to generate an image with 25% of the full count, resulting in images with about 2 times higher noise level (4 times less counts gives about 2 times higher percentage noise).

Image analysis and liver uptake measurements

In the first (HOVON-84) dataset, the liver uptake in all images was analysed in several ways with respect to VOI size and location. Spherical VOIs of 1, 1.5, 2, 3 and 5 cm diameters were placed in the (unaffected) right upper lobe of the livers. In addition, spherical VOIs of 3 cm diameter were placed at different locations within the liver, as illustrated

in Supplementary Fig. 1. Liver SUV_{max}, SUV_{peak} and SUV_{mean} were derived and will be reported as function of VOI size and location. SUV_{peak} was derived according to EANM guidelines using a 1-mL VOI. Moreover, the 3-cm diameter VOI-based liver SUVs were also used to study the impact of imaging time point, i.e. baseline, interim and EoT PET. For the HOVON-84 baseline scans, the total MTV was derived using the fixed SUV_{4.0} threshold, which was recently found to be preferred and robust to assess total tumour burden at baseline in DLBCL [18F]FDG PET/CT studies [20]. The total MTVs obtained were then compared to the observed liver SUV metrics to study if there is an association between liver SUV and tumour load.

For the second and third datasets, we used the 3-cm-diameter VOI placed in the upper right lobe of the liver, as per EANM recommendations. SUV_{max}, SUV_{peak} and SUV_{mean} were reported for each of the applied reconstruction protocols for dataset 2 and measured on the 120 s full and 30 s (25%) count data using dataset 3 and directly compared to demonstrate the impact of reconstruction protocol and noise on liver SUV.

Statistical analysis

Data is described using median values, interquartile ranges (IQR) and is presented using Tukey's boxplots or scatter plots including generalized additive models (GAM) based trend lines. Significance of differences ($p \leq 0.05$) among data was based on paired t tests or Wilcoxon signed rank test, when appropriate. Associations ($p \leq 0.05$) were analysed using Spearman's rank-order correlation testing.

Results

Generally, liver SUV_{max} and SUV_{peak} were 38% and 16% higher in all analyses compared to SUV_{mean}. The effects of VOI size and location are shown in Fig. 1a, b respectively. VOI size mostly affected SUV_{max}, which significant increased up to 31% as VOI size increased (1 vs 3 cm $p < 0.001$, 3 vs 5 cm $p < 0.001$), while SUV_{peak} only increased up to 15%, although significantly (1 vs 3 cm $p < 0.001$, 3 vs 5 cm $p < 0.001$) (Fig. 1a). SUV_{mean} was the only metric that did not show a significant difference among the VOI sizes tested. Moreover, the liver SUV_{max} values were more variable with larger VOI sizes (IQR 0.80 at 1 cm increasing to IQR 1.19 at 5 cm). Contrarily, with increasing VOI sizes an overall decreasing trend in variability was seen when using SUV_{mean} (IQR 0.67 at 1 cm and 0.50 at 5 cm). SUV_{peak} did not show a trend in variability with increasing VOI sizes (IQR 0.60 at 1.5 cm, IQR 0.65 at 1, 2 and 3 cm and IQR 0.74 at 5 cm). The VOI location (Supplementary Fig. 1) did not significantly affect the observed

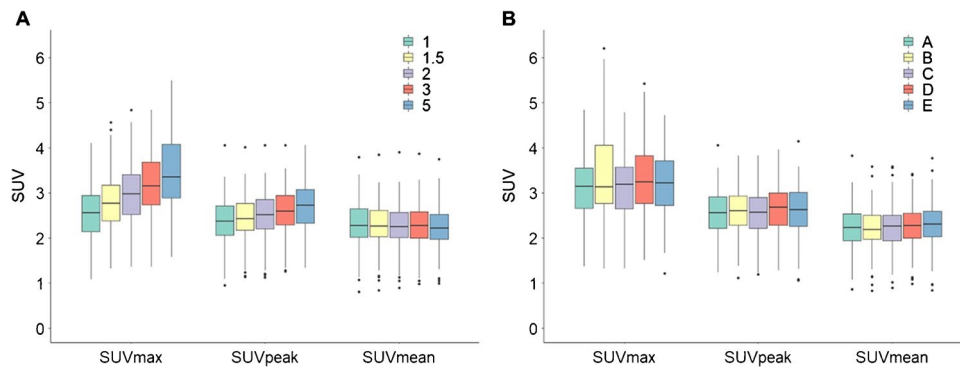


Fig. 1 Liver SUV metrics as function of VOI size (A) and location (B): A SUVmax, SUVpeak and SUVmean per liver VOI size (cm). B SUVmax, SUVpeak and SUVpeak derived per VOI location in liver A-E (as visualized in Supplementary Fig. 1). Central line of the box

is the median, edges of the box are the 25th and 75th percentiles, the whiskers extend to either of the most extreme data points, which are not considered outliers or 1.5 times interquartile range

liver uptake measures (Fig. 1b). The SUVmax values were typically the highest (median ranges 2.6–3.3), followed by SUVpeak values (2.4–2.7) with SUVmean values generally being the lowest (2.2–2.3), regardless of VOI size or location (Supplementary Table 3).

As presented in Fig. 2, a consistent pattern of lower baseline SUV values for each liver uptake metric (SUVmax, SUVpeak and SUVmean) was observed when compared to interim and EoT PET/CT studies. Again, the SUV values differed between the metrics used with overall higher values for SUVmax (median ranges 2.9–3.4), followed by SUVpeak (2.3–2.7) and with the lowest values for SUVmean (2.0–2.4). Likewise, intersubject variability appeared to be largest when using SUVmax (IQR at baseline 1.0, interim 1.1, EoT 0.84) and generally smallest for SUVmean (IQR at baseline 0.62, interim 0.51, EoT 0.55).

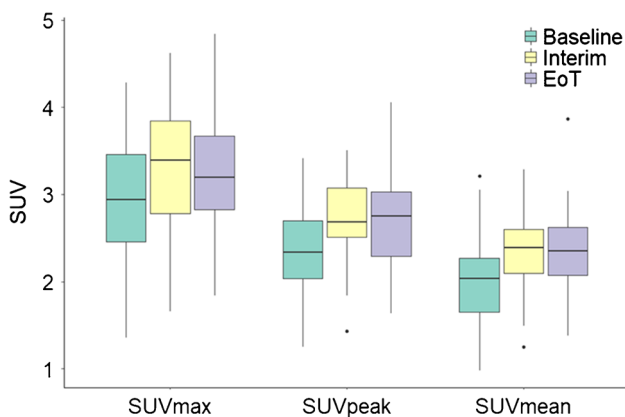


Fig. 2 The effect of treatment time point (i.e. baseline, interim and end-of-treatment) on liver SUV metric values. Central line of the box is the median, edges of the box are the 25th and 75th percentiles, the whiskers extend to either of the most extreme data points, which are not considered outliers or 1.5 times interquartile range

Liver SUV as function of total MTV is illustrated in Fig. 3. For all liver uptake metrics, a trend of decreasing SUV with increasing total MTV can be seen (all $p < 0.05$ using Spearman’s correlation testing) with again the largest intersubject variability when using SUVmax (IQR 1.0) versus SUVpeak (IQR 0.67) and SUVmean (IQR 0.62).

Finally, we studied the impact of reconstruction protocol (EARL-1, EARL-2, 2 mm, 2 mm + PSF) and the effect of image noise by means of scan duration on liver uptake. The liver SUVmax, and to a lesser extent the SUVpeak calculated on the EARL-1 reconstructed scans differed significantly compared to the liver uptake metrics using the other reconstructions (Fig. 4, Supplementary Table 3). The highest median liver SUVmax and SUVpeak values were observed when using 2 mm and 2 mm + PSF reconstructed scans (SUVmax 4.7 and 4.9, SUVpeak 3.2 and

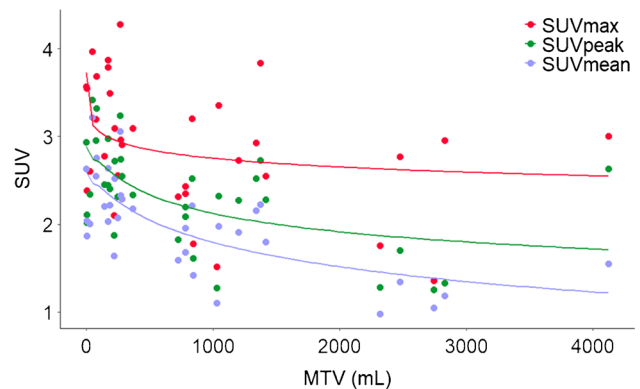


Fig. 3 Liver SUV metric values as function of total metabolic tumour volume (MTV) in milliliter. Solid lines, which are data-driven flexibility curves implementing GAMs (generalised additive models), indicate the general trends

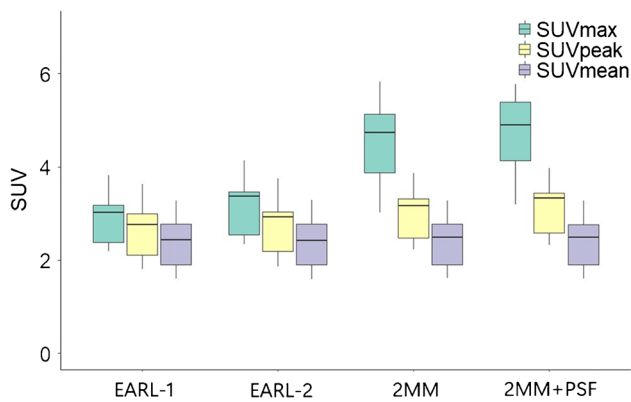


Fig. 4 The effect of reconstruction protocol (EARL-1, EARL-2, 2 mm and 2 mm+PSF) on liver SUV metric values. Central line of the box is the median, edges of the box are the 25th and 75th percentiles, the whiskers extend to either of the most extreme data points, which are not considered outliers or 1.5 times interquartile range

3.3). In particular, the liver SUVmax values appeared to be most variable when derived on the latter reconstructions (IQR 1.26 and 1.27) compared to EARL-1 and EARL-2 (IQR 0.8 and 0.92). Reconstruction protocol barely affected the liver SUVmean values (median of 2.4–2.5). Figure 5 shows liver uptake SUVs measured on the 120 s (100%) and 30 s (25%) per bed position data. There was a clear and significant upward change in liver SUV between the 120 s and 30 s data, respectively, when

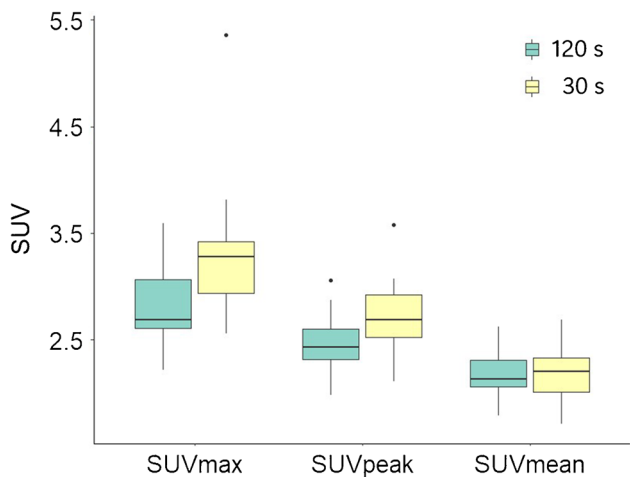


Fig. 5 The effect of image noise (e.g. scan duration) on liver SUV metric values; full count images (120 s per bed position) versus 25% count images (30 s per bed position) images reconstructed on full count images. Central line of the box is the median, edges of the box are the 25th and 75th percentiles, the whiskers extend to either of the most extreme data points, which are not considered outliers or 1.5 times interquartile range

using SUVmax (2.7 and 3.2, $p < 0.05$) and SUVpeak (2.4 and 2.7, $p < 0.05$), but not for SUVmean (2.1 and 2.2, $p = 0.99$).

Discussion

In this study, we aimed to assess whether and to which extent VOI size and location, imaging time point related to treatment phase, tumour load, reconstruction parameters and image noise levels (e.g. scan duration) affect liver uptake measurements and to determine which image analyses approach—in terms of VOI definition and SUV metrics—would provide the most robust and reproducible assessment of liver SUV.

Our findings suggest that SUVmean based on a spherical VOI of 3 cm or larger seems to provide the most robust estimate of the underlying liver SUV, showing limited or no sensitivity for VOI size, VOI location and image noise (e.g. scan duration). Moreover, SUVmean for larger diameter VOIs showed least intersubject variability, most likely because averaging over a larger VOI volume reduces the impact of image noise. This can also be seen when using a 1-cm-diameter VOI (closely equal to the peak VOI definition), showing a similar level of variability as that of SUVpeak. SUVmax is based on a single voxel and therefore most sensitive to noise (increasing when applying PSF and/or smaller voxel size reconstruction and/or shorter acquisition time [17, 21]) resulting in both upward bias as well as increased variability, which was shown previously for tumour uptake measurements as well [16, 19]. The upward bias can be easily understood because with increasing VOI sizes, the probability of finding a noise induced higher maximum value increases, as was explained by Boellaard et al. [21–23].

The exact location of the VOI within the liver appears to have less of an effect on the measured liver SUVs. This is advantageous as usually the VOI is placed by an observer and likely the exact placement of the VOI suffers from intra- and interobserver variability. In our study, the different evaluated locations were well separated such that the translation in VOI placement is much larger than can be expected from any observer when applying clear definitions and rules for placing the VOI, i.e. in the upper right lobe of the unaffected liver. Clearly, locations with image artifacts near the diaphragm due to breathing motion, causing a spatial mismatch between PET and CT for attenuation correction, should be avoided as this will obviously result in inaccurate liver SUV measurements.

Unexpectedly, baseline liver SUVs appear to be lower than those observed at interim and EoT, regardless of the VOI and metric used. In an attempt to explain these findings, we explored the relation between liver SUV and

tumour load by means of total MTV, with the hypothesis that large volume tumours (bulky and/or strongly disseminated) would act as a sink, reducing the availability of [18F]FDG to be taken off by the liver. Indeed, we observed that liver SUVs decrease with increasing total MTV suggesting that baseline tumour [18F]FDG uptake, which is intense and can have large MTVs, may result in lower liver SUV. However, when considering the actual SUVs, these baseline values align with the normal acceptable range suggested in the EANM guideline. Alternatively, it could be hypothesized that interim and EoT liver SUV is elevated due to treatment effects causing extra metabolic activity in the liver. A variety of biological factors potentially affects liver uptake measurements, which are summarized in Supplementary Table 4. The sample size and number of representatives for each potential biological factor in the currently used dataset 1 precludes meaningful analyses of these potential biological biases on liver SUV. The exact cause(s) of the change in SUV with the treatment time points remains unclear, but at least readers should be aware the liver SUV may not remain constant during or after treatment which may have consequences for its use as QC measure, to derive liver SUV-based contouring thresholds or when performing visual or semi-quantitative Deauville scoring.

Based on the findings in this paper we conclude and propose the following recommendations: (1) liver SUV_{mean} is most robust to VOI size, reconstruction protocol and image noise. It therefore reflects the most reproducible liver uptake metric and is recommended when liver uptake is used for QC purposes, as reference for tumour assessment and tumour segmentation thresholding or when it is used as normalisation factor. (2) SUV_{max} shows an upward bias compared to the other SUV metrics in liver as well as in lesions, as was repeatedly shown in several publications [21, 22]. SUV_{max} should therefore not be used for uptake quantification in liver and lesions. (3) Lesional SUV_{peak} seems to be a good surrogate for SUV_{max}, while being less affected by noise and image reconstruction protocol as shown before [16, 17, 19]. SUV_{peak} is nowadays widely available in several image analysis tools and does not depend on the exact tumour contouring method, i.e. minimal or no observer variability as was the main reason to use SUV_{max} before instead of SUV_{mean}. Thus, when using tumour to liver ratio's, we recommend using tumour SUV_{peak} divided by the liver SUV_{mean} based on a VOI size of at least 3 cm in diameter, in order to achieve the most robust and reproducible uptake metrics. (4) Finally, liver SUV is affected by total MTV and/or imaging time point and validity of recommended QC reference ranges may need to be reconsidered or, at least, kept in mind or verified for the specific trial/study at hand.

Conclusions

In this paper, we evaluated the impact of several factors that can affect the liver uptake assessment. Liver SUV_{max} seemed to be most sensitive to VOI size, image noise and reconstruction protocol and should therefore not be used for quality control purposes, to define tumour segmentation thresholds or as reference or normalisation value, i.e. when assessing tumour to liver ratios. Liver SUV_{mean} was most robust against these factors, showing smallest inter-subject variability as well. The commonly recommended liver SUV_{mean} derived from a 3-cm-diameter spherical VOI was only slightly more variable than those seen with larger VOI sizes, which does not seem to justify an urgent adjustment of current guidelines. Finally, we observed that liver uptake may differ systematically between different time points across treatment, possibly caused by the high lesional uptake and large total MTV seen at baseline [18F]FDG PET/CT in DLBCL patients and/or treatment effect which directly affects liver metabolism. This phenomenon should be kept in mind when using liver SUV for any quantitative purpose or when scoring lesion uptakes.

Supplementary Information The online version contains supplementary material available at <https://doi.org/10.1007/s00259-022-05977-5>.

Acknowledgements This work was financially supported by the Dutch Cancer Society (# VU 2018-11648). The sponsor had no role in gathering, analysing, or interpreting the data. The authors thank all the patients who participated in the trial and the HOVON Data Center for collecting the data.

Authors' contributions All authors contributed to the concept and design of the study. M.W.H and R.B were responsible for the statistical design of the study. G.J.C.Z drafted the manuscript. All authors read and approved the final manuscript.

Funding This work is financially supported by the Dutch Cancer Society (# VU 2018-11648).

Data availability The datasets generated during and/or analysed during the current study are available from the corresponding author on reasonable request.

Declarations

Ethics approval and consent to participate The HOVON-84 study (dataset 1, $n = 34$ patients) was approved by the institutional review board of the Erasmus MC (2007-055, NTR1014) and was performed in accordance with the ethical standards as laid down in the 1964 Declaration of Helsinki and its later amendments or comparable ethical standards. Dataset 2 ($n = 15$ patients) and 3 ($n = 15$ patients) are based on (anonymised) data for which retrospective use for technical-scientific purposes was approved by the Medical Ethics Review Committee of Amsterdam UMC, location VUmc (case number VUMC 2018.029) and the need for informed consent was waived [19]. Consultation of the local objection registry verified that none of the selected patients had objected the use of their personal data for research purposes.

Consent for publication Not applicable.

Competing interests The authors declare that they have no competing interests.

Code availability Not applicable.

Open Access This article is licensed under a Creative Commons Attribution 4.0 International License, which permits use, sharing, adaptation, distribution and reproduction in any medium or format, as long as you give appropriate credit to the original author(s) and the source, provide a link to the Creative Commons licence, and indicate if changes were made. The images or other third party material in this article are included in the article's Creative Commons licence, unless indicated otherwise in a credit line to the material. If material is not included in the article's Creative Commons licence and your intended use is not permitted by statutory regulation or exceeds the permitted use, you will need to obtain permission directly from the copyright holder. To view a copy of this licence, visit <http://creativecommons.org/licenses/by/4.0/>.

References

- Barrington SF, et al. Role of imaging in the staging and response assessment of lymphoma consensus of the International Conference On Malignant Lymphomas Imaging Working Group. *J Clin Oncol Official J Am Soc Clin Oncol*. 2014;32(27):3048–58.
- Aide N, et al. EANM/EARL harmonization strategies in PET quantification: from daily practice to multicentre oncological studies. *Eur J Nucl Med Mol Imaging*. 2017;44(Suppl 1):17–31.
- Eertink JJ, et al. (18)F-FDG PET baseline radiomics features improve the prediction of treatment outcome in diffuse large B-cell lymphoma. *Eur J Nucl Med Mol Imaging*. 2022;49(3):932–42.
- Kido H, et al. The metabolic parameters based on volume in PET/CT are associated with clinicopathological N stage of colorectal cancer and can predict prognosis. *EJNMMI Res*. 2021;11(1):87–87.
- Boellaard R, et al. Updating PET/CT performance standards and PET/CT interpretation criteria should go hand in hand. *EJNMMI Res*. 2019;9(1):95–95.
- Boellaard R, et al. FDG PET/CT: EANM procedure guidelines for tumour imaging: version 2.0. *Eur J Nucl Med Mol Imaging*. 2015;42(2):328–54.
- Vali R, et al. SNMMI Procedure Standard/EANM Practice Guideline on Pediatric (18)F-FDG PET/CT for Oncology 1.0. *J Nucl Med*. 2021;62(1):99–110.
- Committee F-PCT *FDG-PET/CT as an imaging biomarker measuring response to cancer therapy*, . Quantitative Imaging Biomarkers Alliance, 2016. Version 1.13, Technically Confirmed Version.
- Eertink JJ, et al. Optimal timing and criteria of interim PET in DLBCL: a comparative study of 1692 patients. *Blood Adv*. 2021;5(9):2375–84.
- Ilyas H, et al. Defining the optimal method for measuring baseline metabolic tumour volume in diffuse large B cell lymphoma. *Eur J Nucl Med Mol Imaging*. 2018;45(7):1142–54.
- Wahl RL, et al. From RECIST to PERCIST: Evolving Considerations for PET response criteria in solid tumors. *J Nucl Med*. 2009;50 Suppl 1(Suppl 1):122s–50s.
- Scheuermann JS, et al. Qualification of PET scanners for use in multicenter cancer clinical trials: the American College of Radiology Imaging Network experience. *J Nucl Med*. 2009;50(7):1187–93.
- Kurch L, et al. Interim PET in diffuse large B-cell lymphoma. *J Nucl Med*. 2021;62(8):1068–74.
- Li YH, et al. The prognostic value of end-of-treatment FDG-PET/CT in diffuse large B cell lymphoma: comparison of visual Deauville criteria and a lesion-to-liver SUV(max) ratio-based evaluation system. *Eur J Nucl Med Mol Imaging*. 2022;49(4):1311–21.
- Kinahan PE, et al. The QIBA Profile for FDG PET/CT as an Imaging Biomarker Measuring Response to Cancer Therapy. *Radiology*. 2020;294(3):647–57.
- Sher A, et al. For avid glucose tumors, the SUV peak is the most reliable parameter for [(18)F]FDG-PET/CT quantification, regardless of acquisition time. *EJNMMI Res*. 2016;6(1):21.
- Kaalep A, et al. Feasibility of state of the art PET/CT systems performance harmonisation. *Eur J Nucl Med Mol Imaging*. 2018;45(8):1344–61.
- Lugtenburg PJ, et al. Rituximab-CHOP with early rituximab intensification for diffuse large B-cell lymphoma: a randomized phase III trial of the HOVON and the Nordic Lymphoma Group (HOVON-84). *J Clin Oncol*. 2020;38(29):3377–87.
- Kaalep A, et al. Quantitative implications of the updated EARL 2019 PET-CT performance standards. *EJNMMI Phys*. 2019;6(1):28.
- Barrington SF, et al. Automated segmentation of baseline metabolic total tumor burden in diffuse large B-cell lymphoma: which method is most successful? A Study on Behalf of the PETRA Consortium. *J Nucl Med*. 2021;62(3):332–7.
- Lodge MA, Chaudhry MA, Wahl RL. Noise considerations for PET quantification using maximum and peak standardized uptake value. *J Nucl Med*. 2012;53(7):1041–7.
- Boellaard R, et al. Effects of noise, image resolution, and ROI definition on the accuracy of standard uptake values: a simulation study. *J Nucl Med*. 2004;45(9):1519–27.
- Mansor S, et al. Impact of PET/CT system, reconstruction protocol, data analysis method, and repositioning on PET/CT precision: an experimental evaluation using an oncology and brain phantom. *Med Phys*. 2017;44(12):6413–24.
- Hasenclever D, et al. qPET - a quantitative extension of the Deauville scale to assess response in interim FDG-PET scans in lymphoma. *Eur J Nucl Med Mol Imaging*. 2014;41(7):1301–8.
- Annunziata S, et al. FDG-PET/CT at the end of immuno-chemotherapy in follicular lymphoma: the prognostic role of the ratio between target lesion and liver SUV(max) (rPET). *Ann Nucl Med*. 2018;32(5):372–7.
- Fan Y, et al. Evaluating early interim fluorine-18 fluorodeoxyglucose positron emission tomography/computed tomography with the SUV(max-liver)-based interpretation for predicting the outcome in diffuse large B-cell lymphoma. *Leuk Lymphoma*. 2017;58(9):1–9.
- Kanoun S, et al. Influence of Software Tool and Methodological Aspects of Total Metabolic Tumor Volume Calculation on Baseline [18F]FDG PET to Predict Survival in Hodgkin Lymphoma. *PLoS One*. 2015;10(10):e0140830.
- Vali FS, et al. Comparison of standardized uptake value-based positron emission tomography and computed tomography target volumes in esophageal cancer patients undergoing radiotherapy. *Int J Radiat Oncol Biol Phys*. 2010;78(4):1057–63.
- Im HJ, et al. Current Methods to Define Metabolic Tumor Volume in Positron Emission Tomography: Which One is Better? *Nucl Med Mol Imaging*. 2018;52(1):5–15.
- Hyun SH, et al. Volume-based parameters of (18)F-fluorodeoxyglucose positron emission tomography/computed tomography improve outcome prediction in early-stage non-small cell lung cancer after surgical resection. *Ann Surg*. 2013;257(2):364–70.
- Eude F, et al. Reproducibility of baseline tumour metabolic volume measurements in diffuse large B-cell lymphoma: is there a superior method? *Metabolites*. 2021;11(2).

32. Malladi A, et al. PET/CT mediastinal and liver FDG uptake: effects of biological and procedural factors. *J Med Imaging Radiat Oncol.* 2013;57(2):169–75.
33. Keramida G, Peters AM. The appropriate whole body metric for calculating standardised uptake value and the influence of sex. *Nucl Med Commun.* 2019;40(1):3–7.
34. Lin CY, et al. Impact of age on FDG uptake in the liver on PET scan. *Clin Imaging.* 2010;34(5):348–50.
35. Cao Y, et al. Age-related changes of standardized uptake values in the blood pool and liver: a decade-long retrospective study of the outcomes of 2,526 subjects. *Quant Imaging Med Surg.* 2021;11(1):95–106.
36. Mahmud MH, et al. Impacts of biological and procedural factors on semiquantification uptake value of liver in fluorine-18 fluorodeoxyglucose positron emission tomography/computed tomography imaging. *Quant Imaging Med Surg.* 2015;5(5):700–7.
37. Liu G, et al. The combined effects of serum lipids, BMI, and fatty liver on 18F-FDG uptake in the liver in a large population from China: an 18F-FDG-PET/CT study. *Nucl Med Commun.* 2015;36(7):709–16.
38. Wang R, et al. Intrapatient repeatability of background (18)F-FDG uptake on PET/CT. *Quant Imaging Med Surg.* 2021;11(9):4172–80.
39. Sprinz C, et al. Effects of blood glucose level on 18F-FDG uptake for PET/CT in normal organs: A systematic review. *PLoS One.* 2018;13(2):e0193140.
40. Kubota K, et al. Effects of blood glucose level on FDG uptake by liver: a FDG-PET/CT study. *Nucl Med Biol.* 2011;38(3):347–51.
41. Keramida G, Peters AM. FDG PET/CT of the non-malignant liver in an increasingly obese world population. *Clin Physiol Funct Imaging.* 2020;40(5):304–19.
42. Webb RL, et al. Effects of varying serum glucose levels on 18F-FDG biodistribution. *Nucl Med Commun.* 2015;36(7):717–21.
43. Viglianti BL, et al. Effect of hyperglycemia on brain and liver (18)F-FDG standardized uptake value (FDG SUV) measured by quantitative positron emission tomography (PET) imaging. *Biomed Pharmacother.* 2017;88:1038–45.
44. Rosica D, et al. Effects of hyperglycemia on fluorine-18-fluorodeoxyglucose biodistribution in a large oncology clinical practice. *Nucl Med Commun.* 2018;39(5):417–22.
45. Iozzo P, et al. Insulin stimulates liver glucose uptake in humans: an 18F-FDG PET Study. *J Nucl Med.* 2003;44(5):682–9.
46. Iozzo P, et al. Quantification of liver glucose metabolism by positron emission tomography: validation study in pigs. *Gastroenterology.* 2007;132(2):531–42.
47. Tenley N, et al. The effect of fasting on PET Imaging of Hepatocellular Carcinoma. *J Cancer Ther.* 2013;4(2):561–7.
48. Nam HY, et al. Concurrent low brain and high liver uptake on FDG PET are associated with cardiovascular risk factors. *Korean J Radiol.* 2017;18(2):392–401.
49. Kamimura K, et al. Associations between liver (18)F fluoro-2-deoxy-D-glucose accumulation and various clinical parameters in a Japanese population: influence of the metabolic syndrome. *Ann Nucl Med.* 2010;24(3):157–61.
50. Liu G, et al. Variations of the liver standardized uptake value in relation to background blood metabolism: an 2-[18F]Fluoro-2-deoxy-D-glucose positron emission tomography/computed tomography study in a large population from China. *Medicine (Baltimore).* 2018;97(19):e0699.
51. Keramida G, et al. Hepatic steatosis is associated with increased hepatic FDG uptake. *Eur J Radiol.* 2014;83(5):751–5.
52. Keramida G, et al. Relationships of body habitus and SUV indices with signal-to-noise ratio of hepatic (18)F-FDG PET. *Eur J Radiol.* 2016;85(5):1012–5.
53. Alexander D, et al. Relationship between regional hepatic glucose metabolism and regional distribution of hepatic fat. *Nucl Med Commun.* 2019.
54. Chen YK, et al. The significance of alteration 2-[fluorine-18] fluoro-2-deoxy-(D)-glucose uptake in the liver and skeletal muscles of patients with hyperthyroidism. *Acad Radiol.* 2013;20(10):1218–23.
55. Yang P, et al. The effect of hypothyroidism on referential background metabolic activity on (18)F-FDG PET/CT. *Quant Imaging Med Surg.* 2021;11(8):3666–76.
56. Lin CY, et al. Positive correlation between serum liver enzyme levels and standard uptake values of liver on FDG-PET. *Clin Imaging.* 2010;34(2):109–12.
57. Chiaravalloti A, et al. Factors affecting intrapatient liver and mediastinal blood pool ¹⁸F-FDG standardized uptake value changes during ABVD chemotherapy in Hodgkin's lymphoma. *Eur J Nucl Med Mol Imaging.* 2014;41(6):1123–32.
58. Oliveira M, et al. Comprehensive analysis of the influence of G-CSF on the biodistribution of (18)F-FDG in lymphoma patients: insights for PET/CT scheduling. *EJNMMI Res.* 2019;9(1):79.
59. Kim SJ, et al. Intra-patient variability of FDG standardized uptake values in mediastinal blood pool, liver, and myocardium during R-CHOP chemotherapy in patients with diffuse large B-cell lymphoma. *Nucl Med Mol Imaging.* 2016;50(4):300–7.
60. Wu X, et al. The association between liver and tumor [(18)F] FDG uptake in patients with diffuse large B cell lymphoma during chemotherapy. *Mol Imaging Biol.* 2017;19(5):787–94.
61. Ceriani L, et al. 18F-FDG uptake changes in liver and mediastinum during chemotherapy in patients with diffuse large B-cell lymphoma. *Clin Nucl Med.* 2012;37(10):949–52.
62. Furuya S, et al. Which is the proper reference tissue for measuring the change in FDG PET metabolic volume of cardiac sarcoidosis before and after steroid therapy? *EJNMMI Res.* 2018;8(1):94.
63. Alin C, et al. Liver standardized uptake value corrected for lean body mass at FDG PET/CT: Effect of FDG uptake time. *Clin Nucl Med.* 2015.
64. Wang R, Chen H, Fan C. Impacts of time interval on 18F-FDG uptake for PET/CT in normal organs: A systematic review. *Medicine (Baltimore).* 2018;97(45):e13122.

Publisher's note Springer Nature remains neutral with regard to jurisdictional claims in published maps and institutional affiliations.